ORIGINAL SCIENTIFIC PAPER

CROATICA CHEMICA ACTA

Croat. Chem. Acta **2023**, *96*(3)
Published online: December 15, 2023
DOI: 10.5562/cca4009

HKD 1926

A Computational Study of the Intermolecular Interactions in the Head-To-Tail Arrangement of the 5CB Liquid Crystal Monomers

Luis Humberto Mendoza-Huizar,[1,*] Eduardo García Sánchez,[2] Luis Octavio Solís Sánchez[2]

[1] Universidad Autónoma del Estado de Hidalgo. Academic Area of Chemistry. Carretera Pachuca-Tulancingo Km. 4.5 Mineral de la Reforma México
[2] Universidad Autónoma de Zacatecas, Unidad Académica de Ingeniería Eléctrica, Av. Ramón López Velarde 801, Zacatecas, 98600, México
* Corresponding author's e-mail address: hhuizar@uaeh.edu.mx

RECEIVED: June 21, 2023 * REVISED: October 29, 2023 * ACCEPTED: November 17, 2023

Abstract: In the present work, we have analyzed the molecular interactions existing in a 4-n-pentyl-4-cyano-biphenyl (5CB) monomer and its dimer, in the head-tail configuration. The optimized geometrical structures of the monomer and dimer were obtained using the theoretical level wB97-XD/6-311G++(d,p). The intermolecular interactions were analyzed through the non-covalent interaction index (NCI) and the localized molecular orbital energy decomposition analysis method (LMO-EDA). Our results suggest that the antiparallel alignment of the 5CB liquid crystal is caused by attractive contributions arising from the intermolecular interactions between the aromatic rings. Furthermore, these interactions were found to cause deformations in the geometries of the monomers forming the dimer.

Keywords: 5CB, dimer, DFT, intermolecular.

INTRODUCTION

LIQUID crystals (LCs) are considered an aggregation state whose properties are intermediate between a crystalline solid and an amorphous liquid.[1–3] In function of their properties, these LCs are being constantly developed, modified, and used industrially in displays, thermometers, light valves, cosmetics, lubricants, ultra-resistant fibers (liquid crystal polymers), films, drugs, and medicines.[4,5] Probably the most commercially important class of LCs to date is 4-alkyl-4'-cyanobiphenyl (CB), because it is used to fabricate displays in calculators, mobile phones, and portable computers.[4,6] 4-n-pentyl-4-cyano-biphenyl (5CB) is one of the LCs most studied because it shows a nematic phase between 297 and 308.3 K. This property allows it to be used in many applications at room temperature.[3] Thus, its properties, such as molecular structure and intermolecular interactions, have been the subject of extensive experimental,[7–15] and theoretical investigations.[7,15–22] These studies include X-ray diffraction,[6,10] IR spectroscopy,[23–25] ultrasonic and Brillouin light scattering,[26] molecular dynamics,[7,18] semiempirical,[27] DFT and MP2 calculations.[17,19] In summary, experimental results reveal that the most preferred dimer arrangement of 5CB is in an overlapping head-to-tail arrangement of neighboring molecules. In this configuration, the dimer is 1.4 times longer than the single monomer.[10,28–30]. Also, this type of alignment has also been identified when 5CB thin films are under confinement. Under these conditions, a parallel orientation of its nematic director to the surface of confinement is called a planar configuration, while a normal orientation of the nematic director corresponds to a perpendicular configuration.[31–33]. In these 5CB thin films, the 5CB dimers formed have a typical thickness of 5 Å and a length of around 25-26 Å.[10,13] Also, similar 5CB configurations have been reported in hybrid systems, where nanosized metal species are included in the dimer.[15]

On the other hand, theoretical studies that employ atomistic potentials have been constructed to successfully describe many of the 5CB key structural motifs, densities, phases, and heats of vaporization.[7,17,34] Amovilli et al. reported a study of the intermolecular interactions in 5CB

dimers by using a two-body potential function derived through the fragmentation reconstruction method (FRM).[17,28] They analyzed the existence of intermolecular interactions in different 5CB configurations, such as parallel face-to-face and side-by-side configurations.[17] However, Amovilli et al. did not analyze the intermolecular interactions for the configuration head-to-tail,[26] which is the most probable experimental geometry.[31,32] Also, it is important to highlight that in these theoretical studies, the intra and intermolecular interactions were fitted empirically to reproduce the experimental and theoretical data, proving the importance of the intra and intermolecular interactions in the prediction of the properties of the 5CB liquid crystal.[34] Nevertheless, an analysis of the origin of such interactions, at the molecular level, has not been performed.[34] We consider that an analysis of the molecular interactions in the 5CB would allow us to clarify the link between its molecular structure and its liquid crystal behavior.[35–37] However, to the best of our knowledge, there is not information, at the molecular level, about the intermolecular interactions in a 5CB dimer in the head-to-tail configuration. We consider that this kind of study is important because intermolecular interactions are directly responsible for the nematic alignment of the 5CB liquid crystal.[10] Therefore, in the present work, we have performed a theoretical quantum study about the intermolecular interactions to gain insight into the behavior of this LC.

METHODOLOGY

In order to find out the optimal geometry during the interaction between two monomers of 5CB, we tested several initial geometries (see Figure 1S in supplementary material) and we perform a conformational search as implemented in Hyperchem.[38] The best structure (minimal energy) was subjected to a full geometry optimization employing the Density Functional Theory. In order to accurately describe the intermolecular interactions in the 5CB dimer ($(5CB)_2$), the dispersion-corrected density functional wB97X-D was used,[39–41] in conjunction with the 6-311++G(d,p) basis set. The Basis Set Superposition Error (BSSE) was estimated using the full counterpoise method.[42,43] The molecular interactions in the optimized $5CB)_2$ dimer were analyzed through the non covalent interactions index (NCI) proposed by Johnson et al.[37] All NCI calculations were obtained with a step size of 0.2 for the cube and a cutoff of 5 Å for the calculation of the interactions. The localized molecular orbital energy decomposition analysis method (LMO-EDA) was used to quantitatively evaluate the contributions to the total interaction energy.[44]

Computational Resources

We used a cluster with 32 cores Xeon 3.0 GHZ and 8 GB of memory for all calculations. These calculations were carried out through the packages Hyperchem,[38] Gaussian 09,[45] GAMESS,[46,47] and visualized with the Gausview,[48] Arguslab,[49] NCIplot,[37] and GNUplot packages.[50]

RESULTS

Intermolecular Interactions in the Monomer 5CB

5CB monomer structure was subjected to a full geometry optimization at the DFT level; prior to the geometry optimization, a conformational search was conducted through the software Hypechem to find the structure of the more stable conformer. In Figure 1, the 5CB monomer structure is depicted, which was optimized at the wB97X-D/6-311++G(d,p) level of theory. Also, the xyz coordinates of the 5CB monomer are reported in Table 1S in the supplementary material. Bond distances and angles are similar to those described in the literature when using a B3LYP/6-31G(d,p) level of theory.[22]

In order to identify the molecular interactions in the 5CB monomer, the NCI index was used.[37] This index is based on the reduced density gradient, s, and the electron density, ρ, see [Eq. (1)].

$$s = \frac{1}{2(3\pi^2)^{1/3}} \frac{|\nabla\rho|}{\rho^{4/3}} \quad (1)$$

s can be plotted against $sign(\lambda_2)$ in a dispersion diagram where $sign(\lambda_2)$ is the second curvature of ρ.[37] In this kind of plot, a spike indicates an interaction. Thus, a spike with a negative sign of λ_2 indicates bonding interactions, which are characterized by a density accumulation perpendicular to the bond. A density depletion is characterized by a positive sign of λ_2, indicating nonbonded interactions.[37] On the other hand, the Van der Waals interactions are identified by a negligible density overlap that gives $\lambda_2 \approx 0$. Thus, the analysis of the sign of λ_2 enables us to distinguish different types of weak interactions, while the magnitude

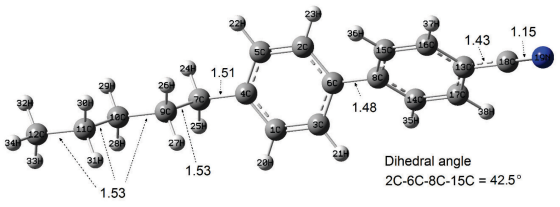

Figure 1. Molecular geometry of 4-*n*-pentyl-4-cyanobiphenyl optimized at the wB97-XD/6-311++G(d,p) level of theory. The bond distances (Å) are labeled in the Figure. Dihedral angles 2C-6C-8C-15C= 42.5° and 9C-7C-4C-5C=-89.4°.

of the electron density measures the strength of the interaction.[37]

Figure 2 shows the plot *s* vs $sign(\lambda_2)$ for the 5CB monomer; note the presence of three spikes. A spike in the negative region indicates a stabilizing interaction, while two spikes in the positive region suggest destabilizing interactions. Also, in this kind of plot, the position, strength, and type of an interaction can be represented through an *s* isosurface, where the signs of λ_2 and electron density size can be related to a color code. The *s* isosurface for 5CB was plotted using electron densities; see Figure 3. Note the presence of two destabilizing interactions in the center of the aromatic rings. From this isosurface, it was not clear whether there were non-covalent stabilizing interactions on the isolated monomer.

Intermolecular Interactions in the $(5CB)_2$ Dimer

It has been reported in the literature that in a nematic liquid crystal, the monomers are restricted to being parallel, following an orientational order.[1] However, in the case of 5CB, the formation of dimers in a parallel head-to-tail configuration has been reported as the most probable experimental geometry.[31,32,51] In order to explore the different three-dimensional arrangements of the 5CB dimer, a conformational search was performed with the help of Hyperchem software.[38] The variation of the torsional angles was allowed to evaluate the energetics of the resulting conformations and identify the most stable conformations. Several initial trial structures were used, as reported in Figure 1S in the supplementary material. In Figure 1Sa, the conformation corresponds to a head-to-head configuration with the central benzene rings in a close perpendicular position. Figure 1Sb shows the head-to-head configuration with the central benzene rings in a close planar alignment position. Figure 1c is the head-to-tail configuration with the central benzene rings in a close perpendicular position, and Figure 1d is the head-to-tail configuration with the central benzene rings in a close planar alignment position. In each case, 1000 conformers per trail structure were requested. In all cases, the more stable conformer corresponds to the head-to-tail configuration with the central benzene rings in planar alignment position (see Figure 1Sd), which agrees with what has been reported in the literature.[31,32,51]

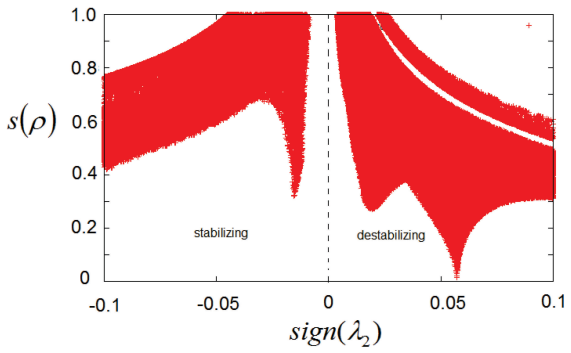

Figure 2. Plot *s* vs $sign(\lambda_2)$ for 5CB monomer.

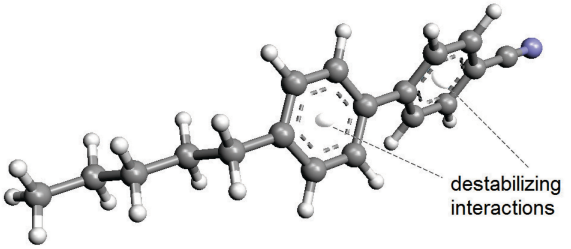

Figure 3. $s(\rho = 0.2)$ isosurfaces of 5CB plotted using electron densities.

Here, it is important to consider that the evaluation of the intermolecular interaction energy depends strongly on the choice of basis set and the electron correlation correction procedure. Therefore, a large basis set near saturation and CCSD(T) level electron correlation correction are necessary for an accurate evaluation of interaction energy between aromatic molecules.[52] In this sense, reports in the literature indicate that the wB97X-D functional is suitable for predicting properties related to non-covalent interactions, such as molecular binding energies and intermolecular distances,[53–56] being able to predict experimental results.[57] Also, the basis set employed, 6-311++G(d,p), includes diffuse and polarization functions, which can adequately describe the long-range interactions as expected in the $(5CB)_2$ dimer. Therefore, we decided to analyze the intermolecular interactions in the $(5CB)_2$ dimer at the wB97X-D/6-311++G(d,p) level of theory. The $(5CB)_2$ structure optimized at this level of theory is depicted in Figure 4. The xyz coordinates of the 5CB dimer are reported in Table 2S in the supplementary material. Note that the 5CB monomers are aligned through the benzene rings. Also, the distance between the ends was measured, and the long axis had a value of 23 Å while the short axis had a distance of 5.3 Å. The monomer length is equal to 16.4 Å, and the length of the $(5CB)_2$ structure is 1.4 times the monomer length, which compares favorably with the obtained experimentally through diffraction pattern measurements.[30,31] Also, the last values compare favorably when the formation of $(5CB)_2$ occurs in an overlapping head-to-tail configuration under confinement conditions where the nematic director of the liquid crystal molecules is aligned with the surface boundary in either a planar or a perpendicular configuration.[30,31] Also, the bond distance values in each monomer of $(5CB)_2$ were measured, and they are similar to the bond distances obtained for the isolated 5CB

monomer; see Figure 1. However, the dihedral angles exhibited by the monomers in the dimer were 2C-6C-8C-15C = –38.7° and 9C-7C-4C-5C = –112.62° for the first one, while 2C-6C-8C-15C = –34.2° and 9C-7C-4C-5C = 128.9° for the second one. Also, in Figure 4, note that there are two small intermolecular interactions between the cyano group and a hydrogen atom located in the opposite monomer with bond lengths of 2.6 and 3.03 Å. The value of these bond lengths suggests a weak interaction that is mostly electrostatic.[58] Thus, even though Onsager's theory suggests that nematic liquid crystals can be modeled as rigid rods,[59] the fact that there are many single bonds with low-barrier torsions in the monomer and dimer indicates that the $(5CB)_2$ dimer should be considered as a flexible rather than a rigid system.

On the other hand, at the wB97X-D/6-311++G(d,p) level of theory, the interaction energy value is –15.7 kcal mol^{-1}. If one does not consider the monomer deformation during the interaction, then the interaction energy is overestimated at –14.0 kcal mol^{-1}.

For $(5CB)_2$, the plot *s* vs *sign*(λ_2) in a dispersion diagram is shown in Figure 5. If one compares this plot with the monomer plot (see Figure 2), it is possible to observe the presence of three new spikes in the negative zone at –0.004,–0.009, and –0.015 while in the positive region, new destabilizing interactions were detected at 0.004, 0.006 and 0.01. In Figure 6, these stabilizing (red) and destabilizing (white) interactions are depicted through an *s* isosurface where the signs of λ_2 and electron density size are color-coded. The stabilizing interactions at -0.015 could be related to a C-ring (center), –0.012 Hydrogen-Ring, –0.009 C(ring)-H(ring), and at –0.004 to the formation of weaker hydrogen bonds, which involve the π-electrons of the triple bond of the cyano group.[60] The destabilizing interactions at 0.01 and 0.004 were related to double bond-ring (center) and double bond-C(ring) interactions. From this figure, it is clear, that the main attractive interactions are located among the aromatic rings. No Nitrogen-Hydrogen bond formation was identified, which is in agreement with recent experimental results.[61]

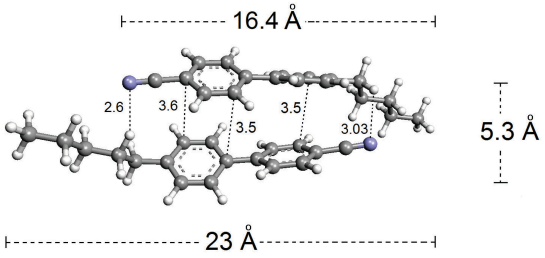

Figure 4. Molecular geometry of $(5CB)_2$ optimized at the wB97X-D/6-311++G(d,p) level of theory. The bond distances (in Å) are labeled into the Figure.

In addition to the NCI study, we analyzed the role of the components that contribute to the total interaction energy through the LMO-EDA method.[62] At the wB97X-D/6-31+G(d) level of theory, the values of the interactions in the 5CB dimer are the electrostatic (–29.63 kcal mol^{-1}), exchange (–1.190 kcal mol^{-1}), dispersion (–15.98 kcal mol^{-1}), polarization (29.65 kcal mol^{-1}) and repulsion (0.016 kcal mol^{-1}) energies. If one analyzes the value of electrostatic interaction, it seems plausible that the largest contribution to the electrostatic attraction would be due to the dipole-dipole interaction. Thus, we evaluated the interaction energy (U) between these dipoles employing the following equation derived for an anti-parallel alignment:[63]

$$U = \frac{-\mu_1\mu_2}{4\pi\varepsilon_0 r^3} \quad (2)$$

where μ_1 and μ_2 are the values of the dipole moments of the monomers 1 and 2, respectively, in the 5CB dimer, ε_0 is the dielectric constant in vacuum and r is the distance between dipoles. As an approximation, we consider the value of $\mu_1 = \mu_2 = 6.92$ D. This value corresponds to the value of the dipole moment for the isolated 5CB monomer evaluated at the wB97X-D/6-311G++(d,p) level of theory.

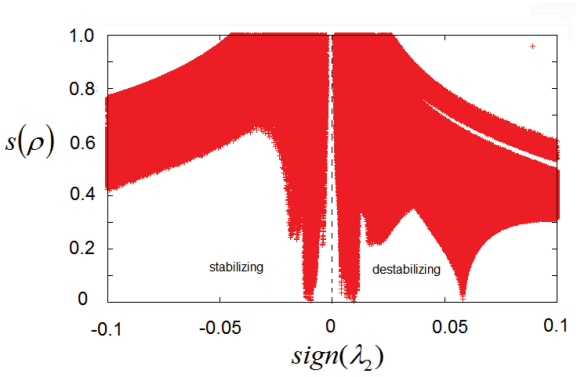

Figure 5. Plot *s* vs *sign*(λ_2) for $(5CB)_2$ monomer.

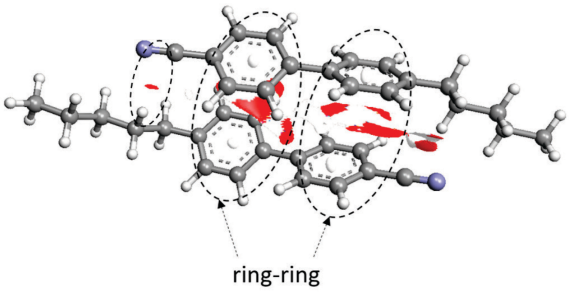

Figure 6. $s(\rho = 0.2)$ isosurfaces of $(5CB)_2$ using electron densities.

The electrostatic interaction energy between dipoles is –19.80 kcal mol^{-1}. If one compares this value with the total electrostatic interaction value (–29.63 kcal mol^{-1}), it is possible to observe that the dipole-dipole interaction is the major electrostatic contribution (67 % approximately) in the dimer. Also, considering all the contributions, the total interaction energy calculated was –17.13 kcal mol^{-1}. These results suggest that the alignment of 5CB monomers in $(5CB)_2$ is caused mainly by the presence of electrostatic, dispersion, and exchange interaction energies. Also, the combination of attractive and repulsive interactions in the center of the molecule contributes to the deformation of the monomers during their interaction.

CONCLUSIONS

In the present study, we have calculated the molecular interactions in a monomer and dimer of 4-*n*-pentyl-4-cyanobiphenyl liquid crystal. The evaluation of the intermolecular interactions employing the NCI index and the LMO-EDA method indicates that the arrangement of the molecules in the 5CB dimer is due mainly to attractive interactions located among the aromatic rings. A combination of attractive and repulsive interactions in different sections of the dimer is causing deformation of the 5CB monomers.

Acknowledgment. L. H. M. H. thankfully acknowledges the computer resources, technical expertise and support provided by the Laboratorio Nacional de Supercómputo del Sureste de México, CONACYT member of the network of National laboratories through the project No. 202203072N and to the Universidad Autónoma del Estado de Hidalgo

Supplementary Information. Supporting information to the paper is attached to the electronic version of the article at: https://doi.org/10.5562/cca4009.

PDF files with attached documents are best viewed with Adobe Acrobat Reader which is free and can be downloaded from Adobe's web site.

REFERENCES

[1] S. Chandrasekhar, *Liquid Crystals*, 2nd ed., Cambridge University Press, **1992**. https://doi.org/10.1017/CBO9780511622496

[2] D.-K. Yang, S.-T. Wu, *Fundam. Liq. Cryst. Devices*. **2006**, 1–37. https://doi.org/10.1002/0470032030.CH1

[3] D. Andrienko, *J. Mol. Liq.* **2018**, *267*, 520–541 https://doi.org/10.1016/J.MOLLIQ.2018.01.175

[4] K. Iwabata, U. Sugai, Y. Seki, H. Furue, K. Sakaguchi, *Molecules,* **2013**, 18, 4703–4717. https://doi.org/10.3390/MOLECULES18044703

[5] Zhang, X. Yang, Y. Zhao, F. Ye, L. Shang, *Adv. Mater.* **2023**, 2300220. https://doi.org/10.1002/ADMA.202300220

[6] M. Ruths, S. Granick, *Langmuir,* **2000**, *16*, 8368–8376. https://doi.org/10.1021/LA000350Z

[7] L. J. Yu, M. M. Labes, *Appl. Phys. Lett.* **1977**, *31*, 719–720. https://doi.org/10.1063/1.89528

[8] G. A. Lambert, *CNS Drug Rev.* **2005**, *11*, 289–316. https://doi.org/10.1111/j.1527-3458.2005.tb00048.x

[9] T. Ikeda, *J. Phys. Chem.* **1990**, *94*, 6550–6555 https://doi.org/10.1021/j100380a008

[10] O. V. Yaroshchuk, Y. P. Piryatinskiĭ, L. A. Dolgov, T. V. Bidna, D. Enke, *Opt. Spectrosc.* **2006**, *100*, 394–399 https://doi.org/10.1134/S0030400X06030143

[11] A. V. Zakharov, M. N. Tsvetkova, V. G. Korsakov, *Phys. Solid State,* **2002**, *44*, 1795–1801. https://doi.org/10.1134/1.1507268/METRICS

[12] L. M. Blinov, V. G. Chigrinov, *Electrooptic Effects in Liquid Crystal Materials* **1994**. Springer-Verlag. New York.

[13] A. R. Noble-Luginbuhl, R. M. Blanchard, R. G. Nuzzo, *J. Am. Chem. Soc.* **2000**, *122*, 3917–3926. https://doi.org/10.1021/ja9939690

[14] N. Lebovka, V. Melnyk, Y. Mamunya, G. Klishevich, A. Goncharuk, N. Pivovarova, *Phys. E Low-Dimensional Syst. Nanostructures.* **2013**, *52*, 65–69. https://doi.org/10.1016/j.physe.2013.03.029

[15] T. I. Shabatina, Y. N. Morosov, *Crystals,* **2020**, *10*, 1–17. https://doi.org/10.3390/cryst10020077

[16] G G. Pelzl, A. Hauser, *Phase Transitions,* **1991**, *37*, 33–62. http://doi.org/10.1080/01411599108203447

[17] A. G. Chmielewski, *Mol. Cryst. Liq. Cryst.* **2011**, *132*, 339–352. http://doi.org/10.1080/00268948608079552

[18] P. Panizza, P. Archambault, D. Roux, R. Effects, *J. Phys. II* **1995**, *5*, 303–311. https://doi.org/10.1051/jp2:1995130

[19] K. L. Mittal, *Polyimides and Other High Temperature Polymers: Synthesis, Characterization and Applications, Volume 3*, CRC Press, **2005** https://doi.org/10.1201/B12194

[20] S. Javadian, N. Dalir, A. G. Gilani, J. Kakemam, A. Yousefi, *J. Chem. Thermodyn.* **2015**, *80*, 22–29. https://doi.org/10.1016/J.JCT.2014.08.010

[21] N. S. Singh, R. Sharma, D. K. Singh, *Enzyme Microb. Technol.* **2019**, *124*, 32–40. http://doi.org/10.1016/J.ENZMICTEC.2019.01.003

[22] D. Sharma, G. Tiwari, S. N. Tiwari, *Pramana - J. Phys.* **2021**, *95* https://doi.org/10.1007/s12043-021-02114-z

[23] M. Bizzarri, I. Cacelli, G. Prampolini, A. Tani, *J. Phys. Chem. A,* **2004**, *108*, 10336–10341. https://doi.org/10.1021/JP047693G

[24] C. Amovilli, I. Cacelli, G. Cinacchi, L. De Gaetani, G. Prampolini, A. Tani, *Theor. Chem. Acc.* **2007**, *117*, 885–901. https://doi.org/10.1007/s00214-006-0209-y

[25] P. K. Chattaraj, *Chemical reactivity theory : a density functional view*, First, CRC Press/Taylor & Francis, Boca Ratón, **2009**

[26] C. Amovilli, I. Cacelli, S. Campanile, G. Prampolini, *J. Chem. Phys.* **2002**, *117*, 3003–3012. https://doi.org/10.1063/1.1494799

[27] S. T. Wu, *J. Appl. Phys.* **1991**, *69*, 2080–2087. https://doi.org/10.1063/1.348734

[28] D. L. Cheung, S. J. Clark, M. R. Wilson, *Phys. Rev. E* **2002**, *65*, 051709 https://doi.org/10.1103/PhysRevE.65.051709

[29] P. Raynes, *Liquid Crystals* — Second Edition, by S Chandrasekhar, Cambridge University Press, **1993**.

[30] L. Longa, W. H. De Jeu, *Phys. Rev. A* **1982**, *26*, 1632 https://doi.org/10.1103/PhysRevA.26.1632

[31] A. J. Leadbetter, R. M. Richardosn, C. N. Colling, *Le J. Phys. Colloq*. 1975, **36,** C1-37–C1-43. https://doi.org/10.1051/JPHYSCOL:1975105

[32] Y.-K. Cho, S. Granick, *Cit. J. Chem. Phys.* **2003**, *119*, 547–554. https://doi.org/10.1063/1.1568931

[33] I. Gnatyuk, G. Puchkovskaya, O. Yaroshchuk, Y. Goltsov, L. Matkovskaya, J. Baran, T. Morawska-Kowal, H. Ratajczak, *J. Mol. Struct.* **1999**, *511–512*, 189–197. https://doi.org/10.1016/S0022-2860(99)00159-3

[34] J. Crain, A. Komolkin, *Simulating Molecular Properties of Liquid Crystals* , in I. (Ilya) Prigogine, S. A. Rice (Eds.), *Adv. Chem. Physics, Vol. 109*, 1st ed., John Wiley & Sons, **1999**.

[35] P. J. Collings, M. R. Fisch, M. A. Mooney, *Am. J. Phys.* **1990**, *60*, 958–958. https://doi.org/10.1119/1.16977

[36] P.-G. de Gennes, J. Prost, *Phys. Liq. Cryst.* Oxford University Press, **1995**.

[37] E. R. Johnson, S. Keinan, P. Mori-Sánchez, J. Contreras-García, A. J. Cohen, W. Yang, *J. Am. Chem. Soc.* **2010**, *132*, 6498–506. https://doi.org/10.1021/ja100936w

[38] Hypercube, Hyperchem ver. 8.08. http://www.hyper.com/. Accessed March 4, **2020**.

[39] J. Da Chai, M. Head-Gordon, *Phys. Chem. Chem. Phys.* 2008, **10,** 6615–6620. https://doi.org/10.1039/b810189b

[40] M. Torbjörnsson, U. Ryde, *Electron. Struct.* **2021**, *3*, https://doi.org/10.1088/2516-1075/ac1a63

[41] N. Mardirossian, M. Head-Gordon, *Mol. Phys.* **2017**, *115*, 2315–2372. https://doi.org/10.1080/00268976.2017.1333644

[42] S. F. Boys, F. Bernardi, *Mol. Phys.* **1970**, *19*, 553–566. https://doi.org/10.1080/00268977000101561

[43] P. Su, H. Li, *J. Chem. Phys.* **2009**, *131*, 014102 https://doi.org/10.1063/1.3159673

[44] Y. Zhao, D. G. Truhlar, *Theor Chem Acc.* **2008**, *120*, 215–241. https://doi.org/10.1007/s00214-007-0310-x

[45] M. J. Frisch, G. W. Trucks, H. B. Schlegel, G. E. Scuseria, M. A. Robb, J. R. Cheeseman, G. Scalmani, V. Barone, B. Mennucci, G. A. Petersson, H. Nakatsuji, M. Caricato, X. Li, H. P. Hratchian, A. F. Izmaylov, et al., **2009**.

[46] M. W. Schmidt, K. K. Baldridge, J. A. Boatz, S. T. Elbert, M. S. Gordon, J. H. Jensen, S. Koseki, N. Matsunaga, K. A. Nguyen, S. Su, T. L. Windus, M. Dupuis, J. A. Montgomery, *J. Comput. Chem.* **1993**, *14*, 1347–1363. https://doi.org/10.1002/JCC.540141112

[47] M. S. Gordon, M. W. Schmidt, *Theory Appl. Comput. Chem. First Forty Years.* 2005. 1167–1189. https://doi.org/10.1016/B978-044451719-7/50084-6

[48] T. Keith, J. Millam, K. Eppinnett et al. Gauss View 05, Dennington II. Inc, Shawnee Mission, KS. **2005**.

[49] M. A Thompson, (**2004**) Molecular Docking Using ArgusLab, an Efficient Shape-Based Search Algorithm and the a Score Scoring Function. ACS Meeting, Philadelphia. http://www.arguslab.com/arguslab.com/ArgusLab.html.

[50] T. Williams, C. Kelley, C. Bersch, H.-B. Bröker, J. Campbell, R. Cunningham, D. Denholm, G. Elber, R. Fearick, C. Grammes, L. Hart, L. Hecking, P. Juhász, T. Koenig, D. Kotz, et al., (**1986**). http://sourceforge.net/projects/gnuplot. Accessed December 19, 2022.

[51] R. Dabrowski, P. Kula, J. Herman, *High birefringence liquid crystals*, **2013.** https://doi.org/10.3390/cryst3030443

[52] R. Hilal, W. M. I. Hassan, A. Alyoubi, S. G. Aziz, S. A. K. Elroby, *Indian J. Chem. - Sect. A Inorganic, Phys. Theor. Anal. Chem.* **2013**, *52*, 19–27

[53] D. Sutradhar, A. K. Chandra, T. Zeegers-Huyskens, *Int. J. Quantum Chem.* **2016**, *116*, 670–680. https://doi.org/10.1002/QUA.25083

[54] T. N. Lohith, M. K. Hema, C. S. Karthik, S. Sandeep, L. Mallesha, N. S. Alsaiari, M. A. Sridhar, K. M. Katubi, K. M. Abualnaja, N. K. Lokanath, P. Mallu, S. R. Kumaraswamy, *J. Mol. Struct.* **2022**, *1266*, 133378 https://doi.org/10.1016/j.molstruc.2022.133378

[55] F. Safdari, H. Raissi, M. Shahabi, M. Zaboli, *J. Inorg. Organomet. Polym. Mater.* **2017**, *27*, 805–817. https://doi.org/10.1007/s10904-017-0525-9

[56] Z. Chen, Y. Li, Z. He, Y. Xu, W. Yu, *J. Chem. Res.* **2019**, *48*, 293–303. https://doi.org/10.1177/1747519819861626

[57] T. Karthick, P. Tandon, K. Srivastava, S. Singh, *Arab. J. Chem.* **2018**, *11*, 591–608. https://doi.org/10.1016/j.arabjc.2017.10.012

[58] S. J. Grabowski, *Hydrog. Bond. - New Insights,* **2006**, 1–520. https://doi.org/10.1007/978-1-4020-4853-1

[59] L. Onsager, *Ann. N. Y. Acad. Sci.* **1949**, *51*, 627–659. https://doi.org/10.1111/j.1749-6632.1949.tb27296.x

[60] P. J. Krueger, H. D. Mettee, *J. Mol. Spectrosc.* **1965**, *18*, 131–140 https://doi.org/10.1016/0022-2852(65)90069-x

[61] T. Bezrodna, V. Nesprava, V. Melnyk, G. Klishevich, N. Curmei, T. Gavrilko, O. Roshchin, J. Baran, M. Drozd, *Low Temp. Phys.* **2023**, *49*, 302–309 https://doi.org/10.1063/10.0017240

[62] P. Su, H. Li, *J. Chem. Phys.* **2009**, *131*, 014102 https://doi.org/10.1063/1.3159673

[63] J. E. Huheey, E. A. Keiter, R. L. Keiter, *Química inorgánica. Principios de estructura y reactividad.*, OXFORD UNIVERSITY PRESS, Mexico, **2009**.